

# The largest scales of turbulent wall flows

By Javier Jiménez<sup>1</sup>

## 1. Introduction

The small scales of wall-bounded turbulent flows have received a lot of attention in recent years, especially in the near-wall region, in part because of the availability of direct numerical simulations that made their detailed study possible (Kim, Moin & Moser 1987). Since those simulations had necessarily moderate Reynolds numbers and little or no separation between their largest and smallest scales, the study of the former independently of the latter in them was difficult. The purpose of this paper is to study the flow scales which are of the order of or larger than the channel width or the boundary layer thickness. We will see that their contribution to the integral flow quantities is not negligible.

The resolution of experiments and simulations is usually adjusted so that the discretized variables are smooth while the size of the numerical box, or of the experimental record, is chosen so that the correlation functions at distances comparable to the box size decay to a negligible level. The latter is intended to guarantee that there is little energy at scales larger than the box size, but it has to be interpreted with care. The energy in a flow that has been low-passed filtered at scales of order  $\lambda$  is proportional to the integral of the correlation function over separations longer than  $\lambda$  and decays slower than the function itself. Since singular spectra such as those in turbulent flows give rise to algebraically decaying correlation tails, it is possible to have correlations which appear to have decayed but which still have a substantial fraction of the energy in their tails.

The peak of the one-dimensional spectrum is moreover typically at  $k = 0$ . This becomes important if the filtered signals are the interesting ones such as in acoustics, where sound attenuation decreases with wavelength and only long waves survive at long distances.

Large structures are also physically interesting because long wavelengths imply long lifetimes and large volumes, and their integrated coherent effect can be comparable to those of the smaller ones even when their power per unit volume is not. Thus if the one-dimensional power spectrum of a signal tends to a constant  $E_0$  as  $k \rightarrow 0$ , the power is contained in wavelengths longer than  $\lambda$  is  $O(E_0/\lambda)$ , but since the lifetime of each structure is proportional to  $\lambda$ , the total energy per structure is independent of the wavelength. As an example, even a small transverse velocity acting for a long time would lead to substantial modifications of the velocity profile. For a flow to be well represented in this sense implies that its resolved spectrum should decay at the lowest wavenumbers as well as at the highest ones, which may never be true in turbulent flows.

<sup>1</sup> Also with the School of Aeronautics, U. Politécnica Madrid.

A less restrictive spectral criterion, involving only considerations of power per unit volume and, therefore, roughly equivalent to the condition on the correlation function, is that the product

$$\phi = kE(k), \quad (1)$$

should decay for the lowest observed wavenumbers since that pre-multiplied spectrum is proportional to the power in a logarithmic band centered at  $k$  (Bullock, Cooper and Abernathy, 1978). Note that the same is true if the wavelength,  $\lambda = 2\pi/k$ , is used in the abscissae instead of the wavenumber since  $d \log \lambda = -d \log k$  and the integral is the same in both cases. In this paper we will generally use  $\phi(\lambda)$ .

There is another reason for studying these largest scales of wall turbulence. We have already mentioned that in some parts of the flow they carry a substantial fraction of the kinetic energy and are, therefore, important by themselves. They may also be simpler to study than regular turbulent structures in the inertial range. Since they are large but their velocity fluctuations are still small compared to the velocity differences in the mean flow, their velocity gradients are weak compared to the mean shear and can be approximately described as quasi-linear. We will in fact see that they share some of the characteristics of rapidly distorted turbulence.

This suggests the appealing possibility that wall flows could be described, as in the case of many free-shear ones, in terms of large-scale quasi-linear structures modulated by essentially isotropic small scales. This would contribute to the unification of an area of turbulence research, the study of the large scales, which has usually been considered non-universal.

## 2. Experimental evidence

### 2.1 Spanwise scales

Almost all the available information on the energy-containing spanwise scales in wall turbulence comes from direct numerical simulations. Spectra from two channels at  $Re_\tau = 180$  (Kim, Moin & Moser, 1987) and  $Re_\tau = 590$  (Mansour, Moser & Kim, 1996) are given in Fig. 1. The spectra of  $u$  and  $w$  near the wall show the well-known peak at  $\lambda_z^+ \approx 100$  corresponding to the spanwise periodicity of the streaks. It is interesting that the wall-normal  $v$  spectrum peaks at a wavelength which is twice shorter than the other two. This was already observed in the transverse correlation functions by Kim *et al.* (1987), who explained it as corresponding to the diameter of the streamwise vortices. That explanation is only partly convincing since it is not clear why it would not apply as well to the spanwise velocity, which is also presumably associated with the vortices. The same effect is, moreover, observed at all distances from the wall, where coherent vortices are not necessarily present, and the effect should probably still be considered unexplained.

As we move away from the wall, the spectral peaks move to longer wavelengths and, near the center of the channel, show signs of being constrained by the periodicity of the numerical box. This is specially noticeable in the  $u$  spectrum of the high-Reynolds number channel, but all the  $u$  and  $w$  pre-multiplied spectra above  $y/h \approx 0.5$  have their maxima at the second numerical wavelength, making it impossible to predict which their behavior would be in a wider box. It is clear, on the

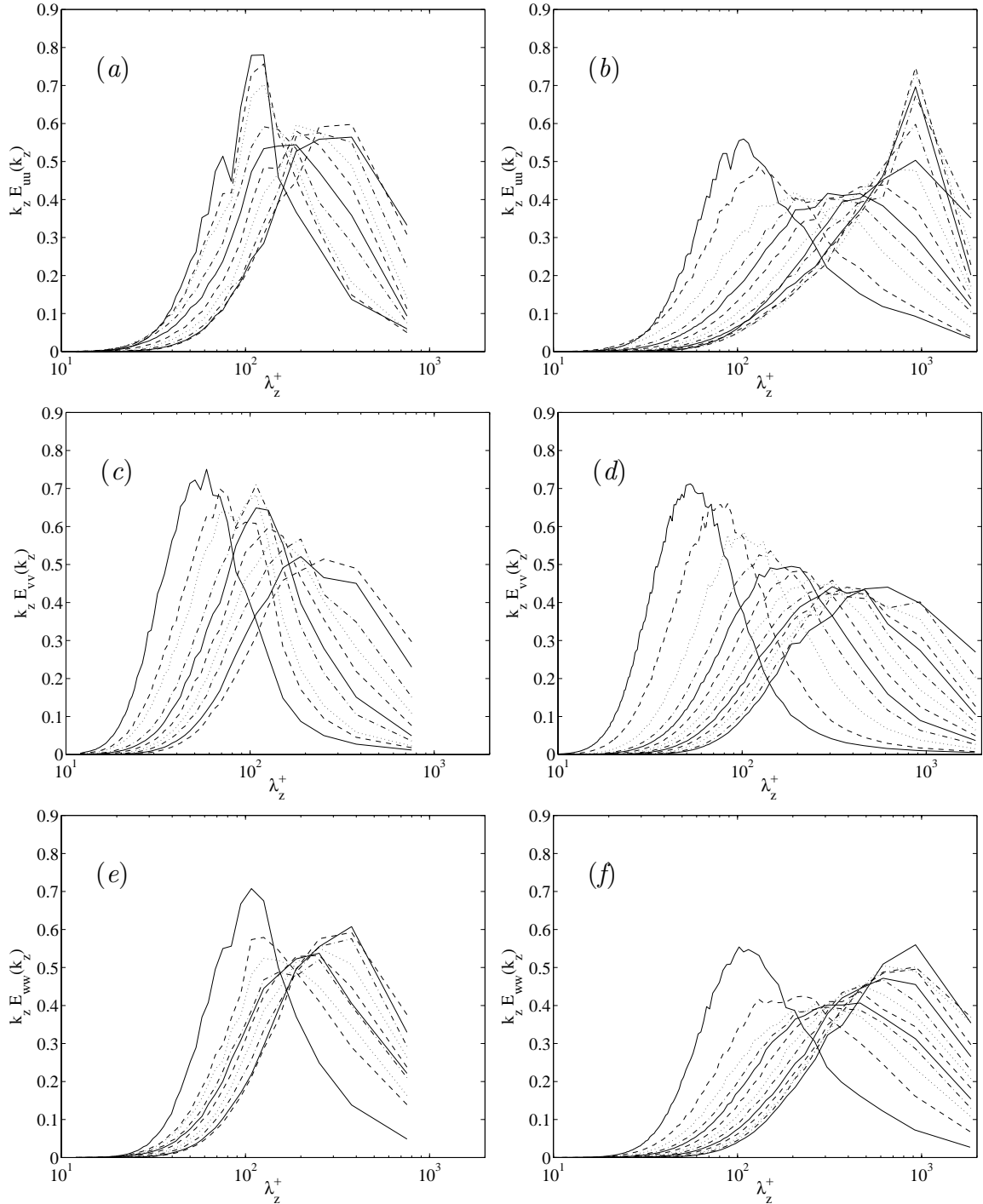


FIGURE 1. Pre-multiplied power spectrum  $k_z E(k_z)$ , as a function of  $\lambda_z^+$ . (a) and (b),  $E_{uu}$ ; (c) and (d),  $E_{vv}$ ; (e) and (f),  $E_{ww}$ . (a), (c) and (e),  $Re_\tau = 180$  channel from Kim *et al.* (1987):  $y^+ = 4, 17, 23, 38, 50, 66, 84, 107, 141, 180$ . (b), (d) and (f),  $Re_\tau = 590$  channel from Mansour *et al.* (1996):  $y^+ = 5, 19, 39, 60, 77, 99, 129, 167, 215, 274, 357, 461, 590$ . In both cases increasing  $y^+$  corresponds to a rightward shift of the short-wavelength end of the spectrum, and lines rotate between solid, dashed, dotted and chaindotted. All the spectra are normalized to unit area, to emphasize their frequency content.

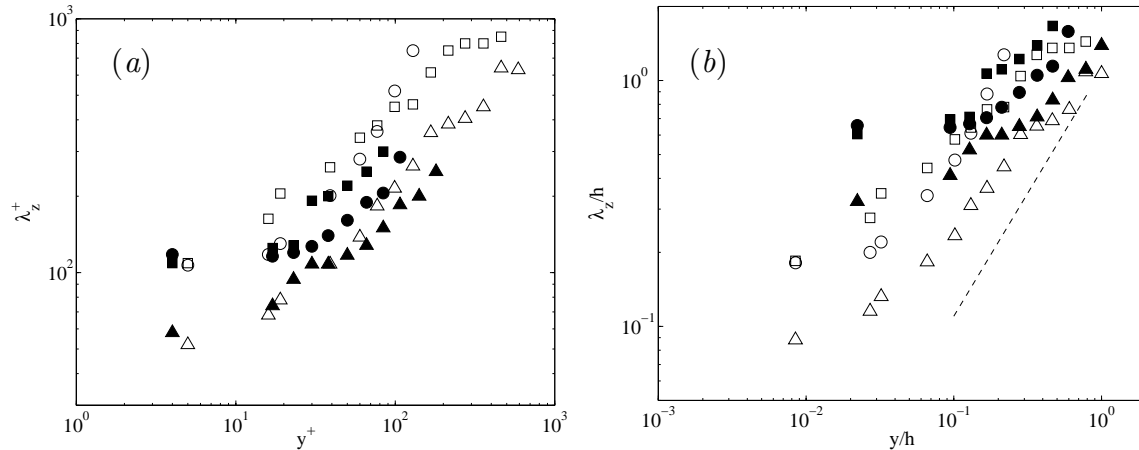


FIGURE 2. Spanwise wavelength of the maxima of the pre-multiplied spectra.  $\circ$ ,  $E_{uu}$ ;  $\triangle$ ,  $E_{vv}$ ;  $\square$ ,  $E_{ww}$ . Open symbols,  $Re_\tau = 590$ ; closed symbols,  $Re_\tau = 180$ . The dashed line has slope 1. (a) Wall units. (b) Outer units.

other hand, that the range of scales at  $Re_\tau = 590$  is wider than at  $Re_\tau = 180$ , suggesting that, since the wavelengths near the wall clearly scale in wall (Kolmogorov) units, those near the center-line probably scale in outer units and are proportional to the channel width.

The spanwise wavelengths of the energy maxima for the different pre-multiplied spectra are given in Fig. 2. They were extracted manually from the data in Fig. 1 and should, therefore, be only taken as rough approximations. Only spectra whose maxima are not in one of the two rightmost points have been used in the figure. It is apparent that the data from both Reynolds numbers collapse very near the wall to approximately 100 wall units for  $E_{uu}$  and  $E_{ww}$  and grow approximately linearly as fractions of the channel height beyond  $y^+ \approx 50$ . The maxima of  $E_{vv}$  follow the same trend but are shorter by roughly a factor of two.

The data from  $v$  have a somewhat longer useful range near the center of the channel although it is clear from the inspection of Fig. 1 that even they should be treated with care. If we take them at face value and assume that their relation with the other two scales holds all the way to the center-line, the maximum size of of the  $v$  structures would be  $\lambda_{zv}/h \approx 1$ , and those of  $u$  and  $w$  would be  $\lambda_z/h \approx 2$ . This agrees with the result of Kim *et al.* (1987) that the velocity correlations decays beyond  $z/h \approx 2$ .

Note that the scales given by these maxima represent the size of the energy-containing structures and are different from the integral scale

$$\lambda_0 = \frac{\pi}{2} \frac{E(0)}{\int_0^\infty E(k) dk}, \quad (2)$$

which can be shown to be roughly proportional to the width of the graph of  $\phi$ , when plotted against  $\log \lambda$ , rather than to its maximum. It is actually easy to construct families of spectra such as

$$E(k) = [1 + a(a - 1)k]e^{-ak}, \quad (3)$$

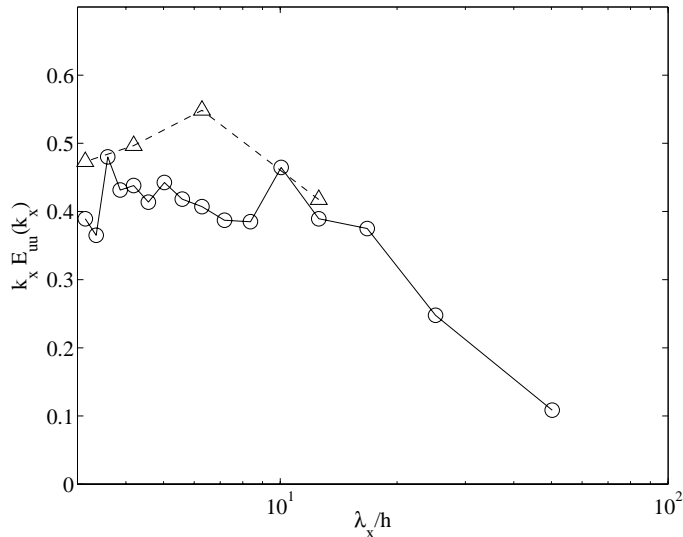


FIGURE 3. Pre-multiplied long-wavelength power spectrum  $k_x E_{uu}(k_x)$  for the pipe in Priymak and Miyazaki (1994) at  $y^+ = 3$ . The dashed line is the spectrum in Kim *et al.* (1987) at  $y^+ = 6$ , included for comparison. Symbols in both cases are the numerical wave numbers.

which have a fixed integral length and an arbitrary location of the energy-containing peak. In this example  $\lambda_0$  is always  $\pi/2$ , while the location  $\lambda_{max}$  of the maximum of  $\phi$  varies from approximately  $2\pi$  for  $a = 1$  to  $\pi a$  for  $a \gg 1$ .

We will later find cases in which the position of the peak is not enough to characterize the energy-containing scales since the spectrum is dominated by an  $E \sim k^{-1}$  range, which appears as a broad plateau in  $\phi(\lambda)$ , but that is not the case here.

## 2.2 Streamwise scales

There is evidence of very long streamwise wavelengths in pipes and channels even if the numerical simulations of Kim *et al.* (1987) show that the correlations decay beyond  $x/h \approx 4$  in the streamwise direction. In this section we will use  $h$  to represent either the half-width of a channel or the radius of a pipe, while  $\delta$  will be reserved for the boundary layer thickness.

Priymak and Miyazaki (1994), using coarse numerical simulations of a low Reynolds number pipe ( $Re_\tau \approx 150$ ), find that their pre-multiplied streamwise spectra have an  $E \sim k^{-1}$  range that only decays beyond  $\lambda_x/h \approx 5\pi$  (Fig. 3). This low-wavenumber behavior was found below  $y^+ \approx 60$  ( $y/h = 0.4$ ). Note that as mentioned above a substantial part of the pre-multiplied spectrum extending beyond the longest resolved wavelength implies that part of the energy is not properly represented.

Bullock *et al.* (1978) found a similar low-wavenumber behavior in their experimental investigation of a turbulent pipe at  $Re_\tau = 2600$ . Their pre-multiplied longitudinal velocity spectra contain two ‘peaks’. The one at the shortest wavelength is at  $\lambda_x^+ \approx 600$  and is the only one present near the wall. Above  $y^+ \approx 60$  another peak appears, or rather a  $k^{-1}$  range develops between the near-wall peak and a mild maximum at low wavenumbers which vary from  $\lambda_x/h \approx 3$  at  $y^+ = 60$  to

$\lambda_x/h \approx 20$  at  $y/h \approx 0.6$ . Beyond this point, the long-wavenumber peak disappears and is replaced by a shorter one at  $\lambda_x \approx h$ , which can be traced to the migration to longer wavelengths of a weakened version of the near-wall peak.

Both wavelength ranges are different. Radial correlations of the streamwise velocity show that the low wavenumbers are correlated across a wide radial range while the high ones are local in the radius.

Perry, Henbest and Chong (1986) made a detailed study of the streamwise  $u$  and  $v$  spectra in smooth pipes with  $Re_\tau = 1, 600 - 3, 900$ , with a special emphasis on the extent and scaling of the  $E \sim k^{-1}$  range. They find that, in the region  $y^+ > 140$  and  $y/h < 0.3$ ,  $E_{uu}$  has a  $k^{-1}$  range which extends between a short-wavelength limit at  $\lambda_x/y \approx 5$  and a longer one at  $\lambda_x/h \approx 15$ . They present no measurements within the near-wall region, but if their short-wavelength limit were extrapolated to the inner edge of the logarithmic layer at  $y^+ \approx 100$ , it would fall in the same range as the near-wall peak mentioned above. Beyond  $y/h \approx 0.3$  the short-wavelength end of the  $k^{-1}$  range is no longer proportional to  $y$  and settles around  $\lambda_x/h \approx 3$ . Although the uncertainties from reading printed spectra are large, the order of magnitude of these wavelengths is comparable to the two ‘peaks’ found by Bullock *et al.* (1978). The marching short-wavelength limit would originate from the near-wall peak and eventually connect with the  $\lambda_x \approx h$  outer peak observed in the center of the pipe by Bullock *et al.*, while the long-wavelength peak would be the same in both experiments. It is interesting that in both cases the  $k^{-1}$  range is only found in what is usually considered the logarithmic region and disappears towards the center of the pipe.

In a previous paper Perry and Chong (1982) had presented results for rough pipes at comparable Reynolds number, although only for  $E_{uu}$  in a narrow range of  $y$  stations within the logarithmic region. The  $k^{-1}$  is very apparent and appears to be longer than in the smooth case. Its long-wavelength limit is at the same location as in the latter, but it extends to shorter wavelengths of the order of  $\lambda_x \approx y$ .

The streamwise spectra for the two numerical channels discussed in the previous section are shown in Fig. 4. There is a clear difference between the spectra of the streamwise fluctuations and those of the other two components. While the latter show only a mild drift to longer scales as they get farther from the wall, the former have most of their energy at very long wavelengths, in agreement with the previous discussion, and are clearly constrained by the numerical box. Note that in the  $Re_\tau = 180$  channel the short end of the  $k^{-1}$  range at the edge of the similarity region would be  $5y^+ \approx 300$ , shorter than the expected viscous length near the wall. As a consequence the position of the spectral peak moves towards shorter wavelengths as it moves away from the wall.

The short-wavelength peak found near the wall in all these cases is probably related to previous observations in experiments and numerical simulations. Clark and Markland (1971) report that the mean streamwise spacing between near-wall vortices is  $\lambda_x^+ = 440$ , while various investigators have reported that the mean distance between substructures within turbulent boundary layer spots is  $\lambda_x^+ \approx 200 - 500$  (see Sankaran *et al.* 1988, and references therein). Jiménez & Moin (1991) observed that

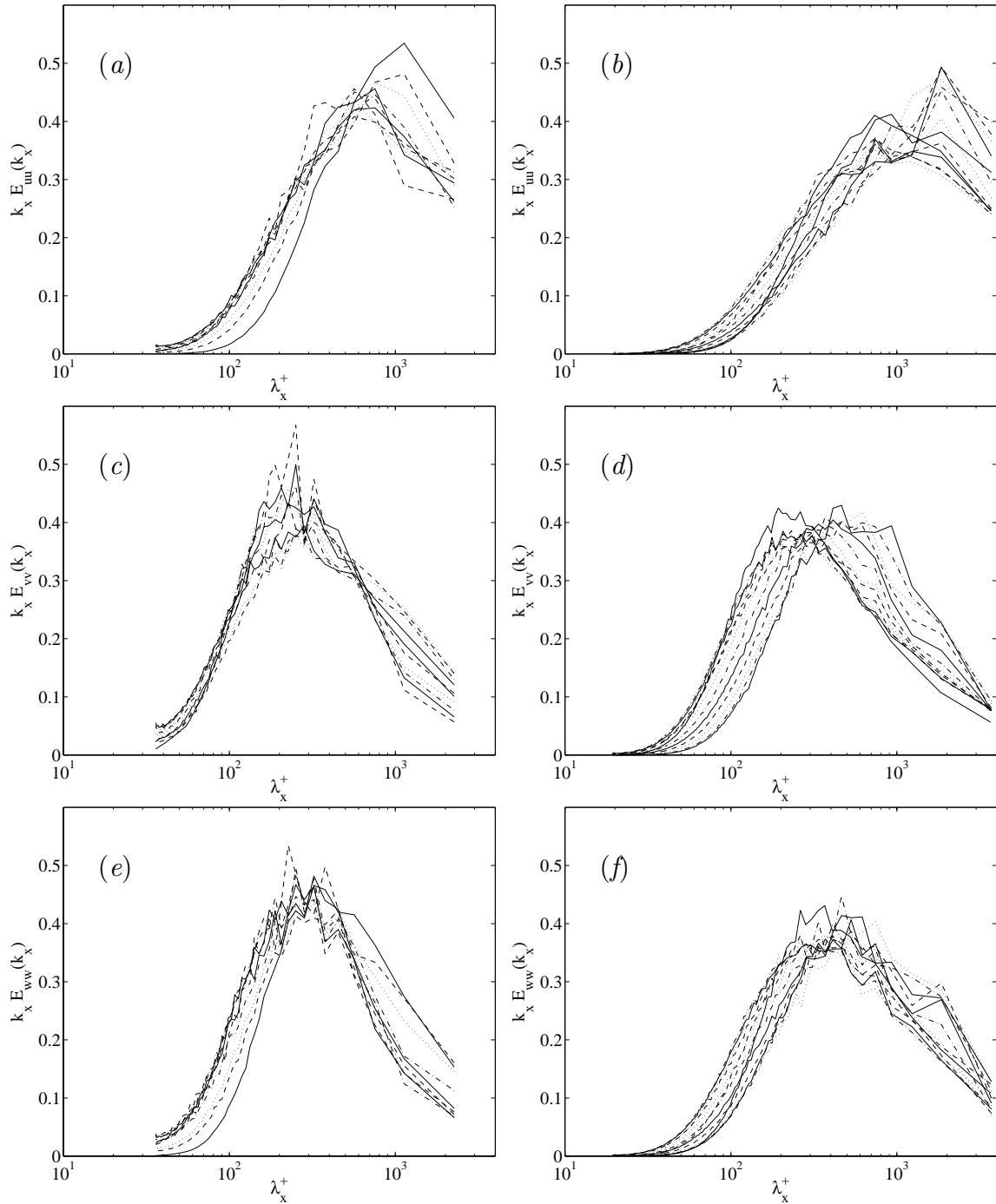


FIGURE 4. Pre-multiplied power spectra  $\phi(\lambda_x)$ . Symbols as in Fig. 1, but in this case the spectra for  $Re_\tau = 180$  move to shorter wavelengths with increasing distance from the wall.

turbulence could not be maintained in numerical boxes with a streamwise periodicity shorter than  $\lambda_x^+ \approx 350$ , while Jiménez & Pinelli (1998) showed that turbulence decays if the streamwise coherence of the velocity streaks near the wall is disturbed

below  $\lambda_x^+ \approx 400$ . In both cases the minimum streamwise period corresponds to boxes containing a single pair of streamwise vortices flanking each sublayer velocity streak.

The long wavenumber range has been reported less often, probably in most cases because of insufficient extent of the numerical or experimental records. Choi and Moin (1990), for example, while studying the wall pressure spectra in the channel of Kim *et al.* (1987), noticed a spurious peak at their lowest wavenumber,  $k_x h = 0.5$  ( $\lambda_x/h = 4\pi$ ), which they attributed to the periodicity of the box, suggesting that the long wavelengths were poorly resolved.

In boundary layers, whose low-wavenumber characteristics need not be identical to those of internal flows, Farabee and Casarella (1991) measured spectra of the wall pressure fluctuations down to very low frequencies. They found that the low-wavenumber end of their pre-multiplied spectra collapses well in outer flow variables and only decreases beyond  $k_x \delta \approx 0.25$  ( $\lambda/\delta \approx 8\pi$ ), where  $\delta$  is a boundary layer thickness roughly equivalent to the pipe radius. Their Reynolds numbers are  $Re_\tau \approx 1,000 - 2,000$ .

Nagib and Hites (1995) and Hites (1997) measured longitudinal velocity spectra in boundary layers with  $Re_\theta = 4 - 20 \times 10^3$ , corresponding to  $Re_\tau \approx 1.5 - 6 \times 10^3$ . They report a  $k^{-1}$  range above  $y^+ = 50$ , extending from a short-wavelength limit at  $\lambda_x^+ \approx 600$  to a longest wavelength of  $\lambda_x/\delta \approx 4$ . The latter is substantially shorter than the long-wavelength limit observed in pipes and channels and also shorter than the wavelength implied by the pressure spectra of Farabee and Casarella (1991). This might be due to a procedural artifact. Their spectra are computed digitally from records which limit them to wavelengths shorter than about  $\lambda_x^+ \approx 10^5$ , which at their highest Reynolds numbers corresponds to  $\lambda_x/\delta \approx 20$ . Since the last few points in the spectrum are generally corrupted by the windowing algorithm, this implies that the location of their low frequency peak is uncertain. It is interesting that their  $k^{-1}$  range is only present below  $y^+ \approx 200$  and that above that range their pre-multiplied spectra contain a single peak at long wavelengths, suggesting again, when compared to other results, that their longest wavelengths may have been missed by the experimental procedure. In fact, in a different analysis of the same data, Hites (1997) measured the fraction of the streamwise kinetic energy in a low-pass filtered version of his velocity signals and found that about 30–50% of the energy was associated with wavelengths longer than the long-wavenumber peak in his spectra and that this fraction increased with the Reynolds number. About 15% was associated with wavelengths longer than  $\lambda_x/\delta = 10$ . This was observed at the only two locations studied in this way,  $y^+ = 100$  and 300.

The experimental results for the longitudinal extent of the streamwise velocity fluctuations are summarized in Fig. 5. Figure 5a gives the location of the short-wavenumber end of the energy-containing range. This is the only longitudinal scale which exists at all positions across the flow. Near the wall it corresponds to an isolated energy peak in the pre-multiplied spectrum near  $\lambda_x^+ \approx 600$ . It grows away from the wall until  $y/h \approx 0.3$ , and it remains constant or decreases slightly above that level. The few data available do not collapse well in either wall or outer units,

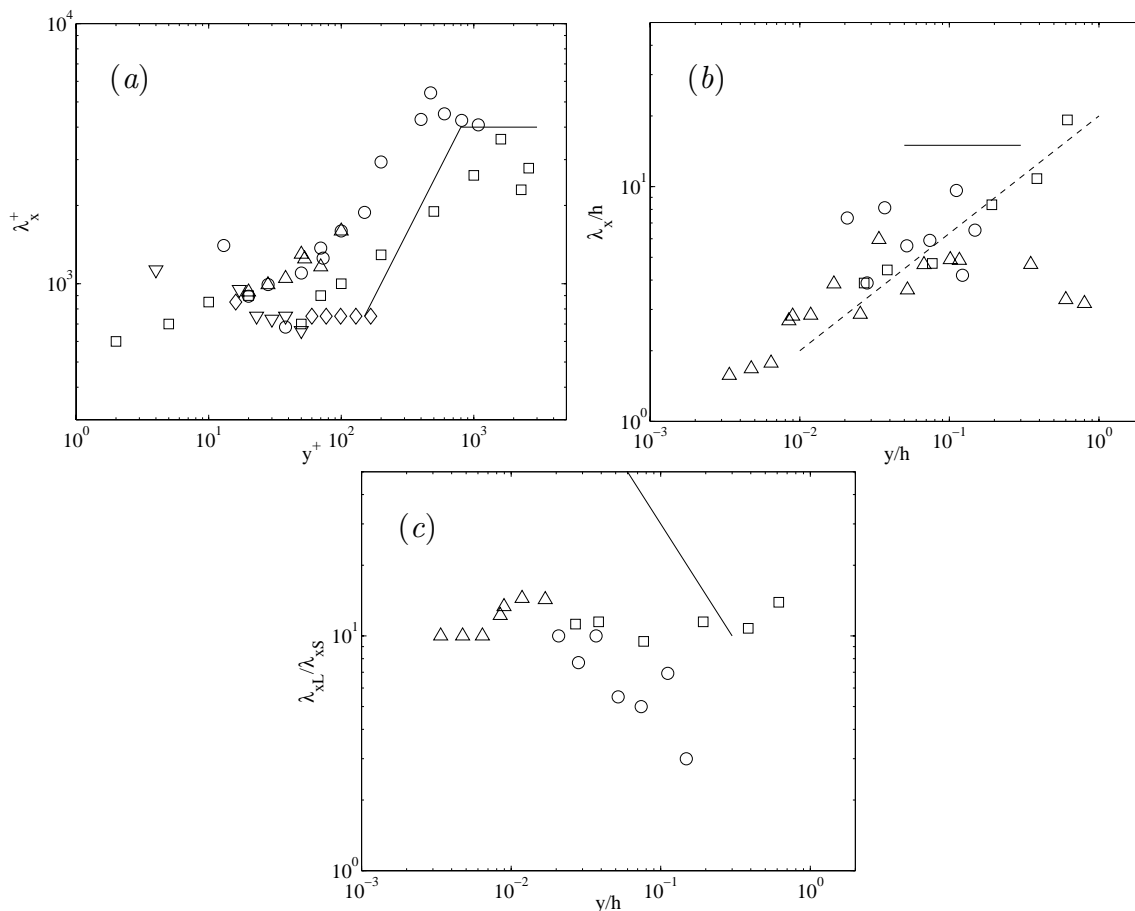


FIGURE 5. Wavelength of the two limits of the  $k^{-1}$  range in  $E_{uu}(k_x)$ , as a function of the distance from the wall.  $\circ$ , Hites (1997),  $Re_\tau = 1350$ ;  $\triangle$ , Hites(1997),  $Re_\tau = 5900$ ;  $\square$ , Bullock *et al.* (1978),  $Re_\tau = 2600$ ;  $\nabla$ , Kim *et al.* (1987),  $Re_\tau = 180$ ;  $\diamond$ , Mansour *et al.* (1996),  $Re_\tau = 590$ ; —, Perry *et al.* (1986),  $Re_\tau \approx 3000$ . (a) Short-wavelength limit in wall units. (b) Long-wavelength limit, in outer units. The dashed line has slope 1/2. (c) Ratio between the two limits of the energy-containing range.

and the support for a linear growth with wall distance is only moderate. The range of useful experimental Reynolds available is not large,  $Re_\tau = 1,000 - 6,000$ , but in that range the maximum wavelength of this peak near the center of the channel is  $\lambda_x/h = 1 - 2$ . We have seen in the previous section that the spanwise extent of the structures containing the streamwise kinetic energy varies from  $\lambda_z^+ = 100$  near the wall to  $\lambda_z \approx 2h$  at the center. Assuming that the structures involved are the same in both cases, this would imply that the large scales vary smoothly from a streamwise aspect ratio of about 6 near the wall to approximate isotropy near the center.

The real picture is more complicated. Between  $y^+ \approx 100$  and  $y/h \approx 0.3 - 0.5$  a second limit appears, which is given in Fig. 5b. It scales well in outer units within the present range of Reynolds numbers and constitutes the long-wavelength limit

of an  $E \sim k^{-1}$  spectral range which contains essentially all the streamwise kinetic energy. The available data, except for those in Perry *et al.* (1986), suggest that the ratio between those two limits is always approximately equal to 10 (Fig. 5c) and that both scales grow as  $y^{1/2}$ . The long-wavelength limit disappears in the center of the channel, and the  $k^{-1}$  range again collapses to a single spectral peak. The existence of the  $k^{-1}$  range approximately coincides in these experiments with the logarithmic region of the mean velocity profile.

The square-root dependence on wall distance is surprising and would imply that the length scale is determined by some viscous mechanism, probably based on an eddy viscosity which stays constant across the flow. This would be difficult to understand, and there is enough scatter in the data to leave open the possibility of a linear dependence, but this is one of the many points in these data that call for urgent clarification.

The data on the other velocity components are scantier. The wall-normal component  $v$  has been measured in several occasions, and there is general agreement that it does not contain a  $k^{-1}$  range (Perry *et al.*, 1986). The  $k^{-5/3}$  inertial range in its one-dimensional streamwise spectrum connects directly with a low-frequency range which is essentially flat. The corner between the two regimes is at about the same scale as the short-wavelength end of the  $k^{-1}$  range in  $E_{uu}$ , and it is at those scales that most of its energy is concentrated. The data in Fig. 4 support this interpretation.

There are even less data on the spanwise component  $w$ . The numerical data in Fig. 4 suggest that there is no  $k^{-1}$  spectrum for this component and that its characteristic wavelengths are those of  $v$  rather than  $u$ . The same can be deduced from the spectra given by Lawn (1971), in a pipe at  $Re_\tau \approx 2,000$ . Although his spectra are noisy and clearly truncated at low frequency, they fall in two groups: long ones for  $E_{uu}$ , which continue growing at his lowest measured frequencies, and short ones for  $E_{vv}$  and  $E_{ww}$ , which flatten beyond  $\lambda_x/h \approx 2$ .

Perry, Lim and Henbest (1987) suggest that  $E_{ww}$  has a short  $k^{-1}$  range in contrast to  $E_{vv}$ , but inspection of their data reveals that if this range exists it is much narrower than that of  $E_{uu}$  and is located at wavelengths which are an order of magnitude shorter than those of  $u$ .

Saddoughi & Veeravalli (1994) and Saddoughi (1997) made measurements in rough perturbed boundary layers at  $Re_\tau = 30,000 - 160,000$ . Although their analysis is centered on the isotropy of the inertial range, the long-wavelength behavior of their spectra can be used as a check of the Reynolds number independence of the previous conclusions since their  $Re_\tau$  are at least an order of magnitude larger than those discussed up to now. Their spectra also fall clearly in a short group for  $v$  and  $w$  and a long one for  $u$ .

### 2.3 Reynolds stresses

Perry *et al.* (1987) suggest, mostly on theoretical grounds, that no  $k^{-1}$  range should be found in the  $E_{uv}$  cospectrum. The basic argument, which goes back to Townsend (1976) and which is implicit in the classical distinction between ‘active’ and ‘inactive’ motions, is that, since Reynolds stresses depend on the presence of  $v$ ,

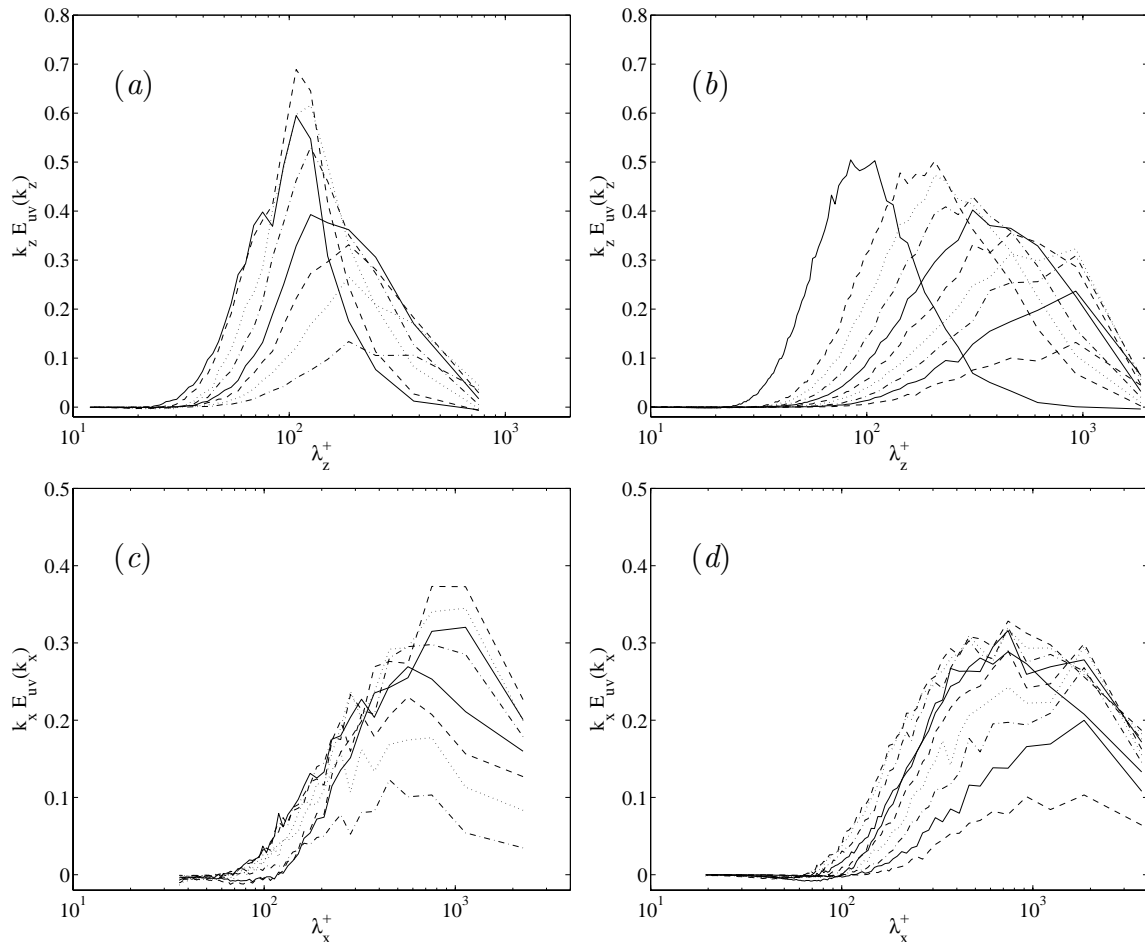


FIGURE 6. Pre-multiplied power co-spectra. (a) and (b)  $k_z E_{uv}(k_z)$ , as a function of  $\lambda_z^+$ . (c) and (d)  $k_x E_{uv}(k_x)$ , as a function of  $\lambda_x^+$ . (a) and (c)  $Re_\tau = 180$  channel from Kim *et al.* (1987):  $y^+ = 17, 23, 38, 50, 66, 84, 107, 141$ . (b) and (d),  $Re_\tau = 590$  channel from Mansour *et al.* (1996):  $y^+ = 16, 60, 77, 99, 129, 167, 215, 274, 357, 461$ . In both cases lines rotate between solid, dashed, dotted, and chaindotted. The spectra are not normalized to unit area, and decreasing amplitudes generally correspond to larger distances from the wall. Note that, as for the velocity spectra in Fig. 4a, the scale of the  $Re_\tau = 180$  cospectrum in (c) decreases away from the wall.

they can not be present at scales at which the latter is not active. A little thought reveal that this is not necessarily so. Consider the low-frequency spectral range in which  $E_{uu} \sim k^{-1}$  and  $E_{vv} \sim 1$ . The only limitation for the cospectrum is that  $E_{uv}^2 \leq E_{uu}E_{vv}$ , and it is possible to have substantial Reynolds stresses even at wavenumbers at which the  $v$  spectrum is already constant.

The streamwise and spanwise cospectra from the two numerical channel simulations are given in Fig. 6. The drift in  $\lambda_z$  away from the wall is similar to that of  $u$  and  $w$  in Fig. 1, and there is a clear suggestion of a  $k_x^{-1}$  range in the streamwise cospectrum of the higher Reynolds number case. A comparison with Fig. 4 shows

that the characteristic wavelengths of the cospectra are those of  $u$  rather than those of  $v$ .

Krogstad, Antonia and Browne (1992) give spectra for  $E_{uu}$ ,  $E_{vv}$ , and  $E_{uv}$  in a boundary layer at  $Re_\tau \approx 2,000$ . The pre-multiplied  $E_{uu}$  and  $E_{uv}$  have broad maxima, both of which only decay beyond  $\lambda_x/\delta \approx 6$ , while  $E_{vv}$  has a narrower peak at wavelengths which are an order of magnitude shorter.

Saddoughi & Veeravalli (1994) measured  $E_{uv}$  at  $y/\delta = 0.1$  and  $0.4$ . The cospectra at the near-wall station have a well-developed  $k_x^{-1}$  range that extends from  $\lambda/\delta \approx 0.5$  to  $\lambda/\delta \approx 7$ . Note that these values are very close to the limits of the  $k_x^{-1}$  range for  $E_{uu}$  given in Fig. 5 at this distance from the wall. Their cospectra at the mid-layer location have essentially no  $k^{-1}$  range.

Lawn (1971) measured some cospectra. They are generally short, like  $v$  and  $w$ , but it is interesting that the two cospectra for which  $y^+ > 200$  and  $y/h < 0.5$  are ‘long’ and continue to increase beyond their lowest wavenumber  $\lambda_x/h = 50$ .

### 3. Discussion

The general picture suggested by the data discussed above is that there exist in the region of the flow generally associated with a logarithmic velocity profile very long structures with longitudinal aspect ratios of the order of 10, which essentially consist of streamwise velocity fluctuations. They contain most of the streamwise kinetic energy. Spanwise and wall-normal velocities have shorter wavelengths, roughly coincident with the shorter end of the scales of the  $u$  structures, and are only slightly elongated in the streamwise direction.

Long streamwise structures which contain predominantly streamwise velocity can best be described as a system of longitudinal jets and are reminiscent of the sublayer low- and high-velocity streaks, although in this case they would clearly be turbulent themselves. In the sublayer streaks, for example, the quasi-streamwise vortices responsible for the  $v$  and  $w$  fluctuations are also shorter than the streaks, and the latter are the result of the action of several vortex pairs (Jeong, Hussain, Schoppa & Kim 1997).

In Fig. 7 we give an instantaneous picture of the  $u$  and  $v$  contours for a wall-parallel plane of the numerical  $Re_\tau = 590$  numerical channel from Mansour, Moser and Kim (1996), even if we have seen that their box is too short to represent these structures correctly. There is clearly a large low-velocity streak on the upper half of the  $u$ -plane which is not present in  $v$ . The transverse section in the lower frame of the figure shows that this is not an isolated case and that there are several jets at roughly the same scale. They are distinct from the sublayer streaks, being much larger, but they seem to form from the joint effect of several of them.

Komminaho, Lundblad, and Johansson (1996), who have observed streamwise structures of the order of  $40h$  in low-Reynolds-number Couette flow, publish snapshots of their simulations which look strikingly similar to Fig. 7.

Very large streaky features with widths and heights of several hundred meters are known to occur in the atmospheric boundary layer, apparently associated with storms having a large geostrophic shear (J. C. R. Hunt, private communication), and

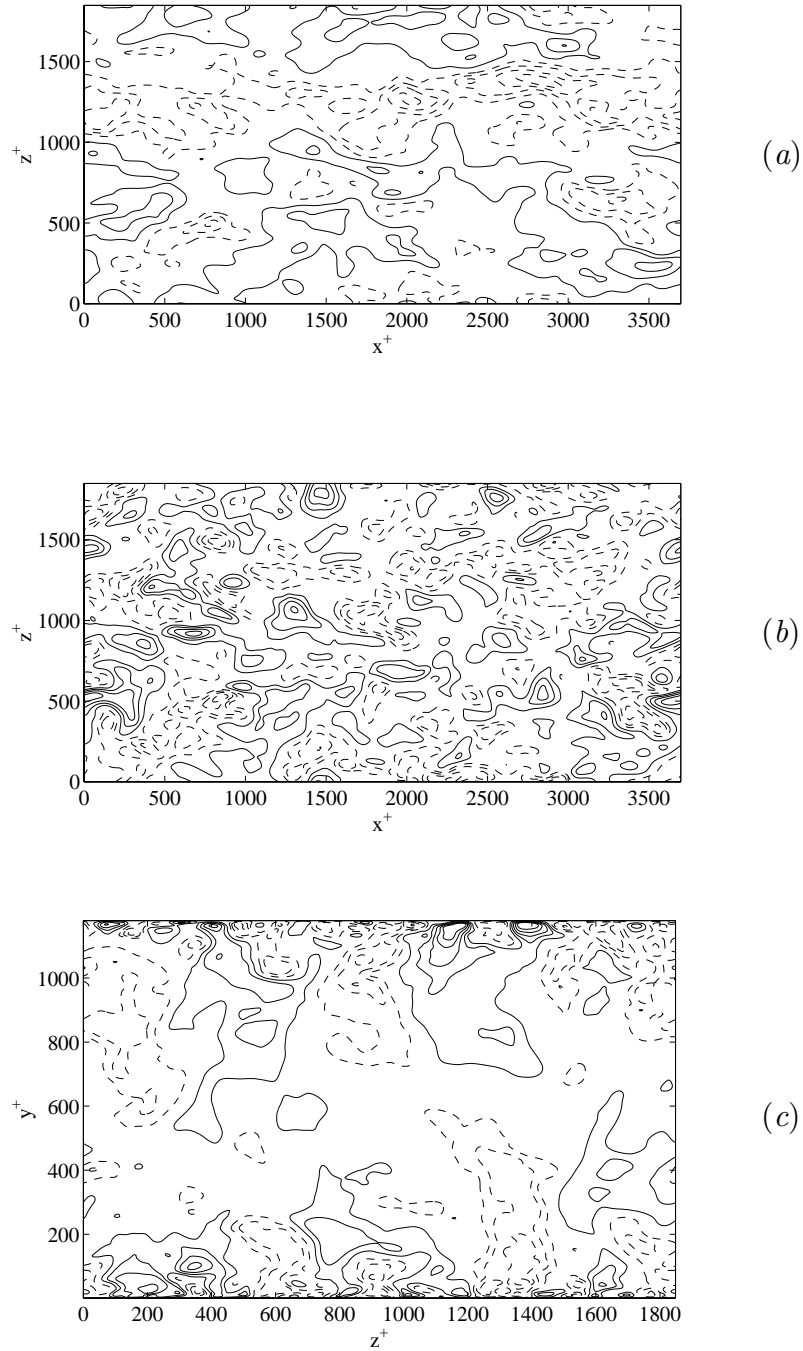


FIGURE 7. Instantaneous filtered velocities in the channel of Mansour *et al.* (1996),  $Re_\tau = 590$ . (a) and (b):  $y^+ \approx 300$  from the lower wall. Flow is from left to right. Velocities are filtered by averaging on a  $13^3$  stencil ( $\Delta x^+ \times \Delta y^+ \times \Delta z^+ \approx 130 \times 75 \times 60$ ). (a) Streamwise velocity fluctuations; contours are  $u' = \pm 0.75(1)$ . Negative contours are dashed, and the fluctuations are computed with respect to the instantaneous mean velocity on the  $x$ - $z$  plane. (b) Wall-normal velocity; contours are  $v' = \pm 0.375(0.5)$ . (c) Transverse section of  $u'$  at  $x^+ \approx 2500$ . Fluctuations, filter and contours as in (a), but there is no filtering in  $y$ .

have been observed underneath tropical hurricanes (Wuman and Winslow, 1998). Smaller scale features, although still much larger than sublayer streaks, are observed in wind-blown sand in beaches (Jiménez, personal observation), and in blowing snow in snow fields (Adrian, private communication).

Perry *et al.* (1986) describe their results in terms of an ‘attached eddy’ model which is an elaboration of an earlier one proposed by Townsend (1976). Briefly, in the logarithmic region, the  $v$  structures are blocked by the presence of the wall and are constrained to sizes at most of order  $y$ . This argument has been extended by Hunt (1984) to any turbulent flow in the presence of a wall, independently of the presence of shear, and to wall-normal correlations lengths. These blocked eddies would form the ‘short’  $\lambda_x \sim y$  peak in both  $v$  and  $u$ . A similar peak would also be expected to appear in  $\lambda_z$ , and we saw evidence for it in Fig. 2. For the tangential components there is no blocking effect, and much larger structures are possible. The peak at  $\lambda \sim y$  would only constitute a short-wavelength limit for them, and one could expect a range of eddies, large in the tangential directions but attached to the wall in the wall-normal one. Perry *et al.* (1986) give a very specific model for these eddies as attached hairpin vortices and use it to derive the  $k^{-1}$  form of the spectrum. The latter behavior is, however, more general than the hairpin model and can be derived from simple dimensional considerations for near-wall structures that are so large that their distance to the wall should not be important (Perry and Abell, 1977).

We have mentioned in the introduction that the internal velocity gradients associated with these large structures are so low that their dynamics should be dominated by the shear in the mean velocity profile. They can, to a first approximation, be considered linear and described by rapid distortion theory. The blocking of  $v$  mentioned above is one such linear effect, but it is independent of the mean shear and depends only on the presence of an impermeable wall. It is easy to see that the effect of a mean shear is that any initial turbulence gets deformed into a series of streamwise jets. In essence, any spectral component with a non-trivial dependence on  $x$  gets damped by the shear, and only the  $x$ -independent motion in the cross-plane is left. This transverse motion depends on the initial conditions and is uncoupled from the streamwise velocity. Except for viscosity, which would be negligible at these large scales, it is undamped and will last for long times. The  $u$  component is transported by this transverse velocity as a passive scalar (Orlandi and Jiménez 1994). Wherever  $v$  moves towards the wall,  $u$  increases, and vice versa. Even if the transverse flow is weak, the modulation of  $u$  increases linearly in time and will grow to form large amplitude longitudinal jets until either viscosity or nonlinear effects halt the growth. It was shown by Orlandi & Jiménez (1994) in the context of ‘laminar’ near-wall streaks that this processes changes the mean velocity profile and, therefore, carries Reynolds stresses.

#### 4. Conclusions and open questions

We have shown that eddies with streamwise lengths of the order of 10–20 boundary layer thicknesses are present in the logarithmic region of wall-bounded flows.

They contain a substantial fraction of the streamwise kinetic energy and, probably, also of the Reynolds stresses. They can be approximately visualized as a system of streamwise turbulent jets, roughly comparable to the sublayer velocity streaks at a much larger scale.

We have given arguments that they should be describable to a first approximation by the combined linear effects of the blocking by the wall and of the mean shear. The first effect has been treated, for example, by Hunt (1984), who showed that it explains the difference between  $v$  and the two tangential spectra. In the absence of a mean shear, there should be no difference in the behavior of the  $u$  and  $w$  spectra, both of which should be ‘large’. We have shown that shear breaks that symmetry and leads directly to longitudinal jets and to a  $u$  spectrum which is much longer than the one for  $w$ .

The appeal of this argument is that it provides some unification to the arguments on the largest scales of turbulent flows. It has been understood for some time that the large structures of *free* shear flows correspond closely to the most unstable eigenfunctions of their mean velocity profiles (Cimbala, Nagib and Roshko, 1988; Gaster, Kit and Wygnanski, 1985). This explanation does not work for wall-bounded flows, whose profiles are typically stable, but it is easy to convince oneself that the linear mechanism described at the end of the last section is nothing but the result of the neutrally-stable Squire’s modes of the inviscid Rayleigh stability equation for the mean profile (Betchov and Criminale 1967).

A unified theory for all these largest structures would treat them as solutions of the linear, inviscid stability equations. If an unstable eigenvalue exists, it dominates the initial value problem. Otherwise, the linearly growing Squire’s modes prevail.

As satisfying as that conclusion might be, it is clear that it should only be considered a preliminary step of a wider work program. Many questions are left unanswered.

Some of them are experimental. There is essentially no information on the spanwise structure of these large scales. We lack experimental data, and the Reynolds numbers of the numerical simulations are too low to draw scaling conclusions. The data on the streamwise scales is better but partially contradictory. Most of the available high Reynolds number experiments either lack spectral information, have too few  $y$ -stations, or have data records which are too short to capture the largest scales. The situation is specially bad for the spanwise velocity component  $w$  and for the cospectrum, for which contradictory interpretations exist.

Except with the use of massive probe rakes it is unlikely that experiments would give geometrical information about the structure of these eddies. Numerical simulations should help, but the twin requirements of very long boxes and high Reynolds numbers make direct simulations difficult. It should be possible, however, to attempt large eddy simulations of a few cases to clarify both the scaling and the geometry.

On the theoretical side, the linear model outlined above is clearly only a first approximation. Nonlinearity has to be taken into account although, hopefully, only as a secular perturbation. In free shear flows it appears in the form of Reynolds

stresses that modify the mean profile responsible for the instability. This is probably the root of the ‘marginal instability principle’ used by Lessen (1978) and co-workers to explain some of their properties. This nonlinear mechanism does not work in wall flows because the mean profile does not feed back into the transverse velocities of the Squire’s modes. Weakly nonlinear models of the near-wall streaks have been proposed by Waleffe (1997) and others, and they could perhaps be adapted to the present case. A cycle for the generation of large streamwise structures in a turbulent profile was proposed by Townsend (1976).

Two especially troublesome aspects of the experiments are related to the question of nonlinearity. The first is the difference of about a factor of 2 between the observed spanwise wavelengths of  $v$  and of the other two velocity component (see Figs. 1 and 2). It is difficult to explain it as a linear property. The second is the apparent  $y^{1/2}$  scaling of the longitudinal scales in Fig. 5 and the corresponding finite range of wavelengths associated with the  $k^{-1}$  range, which is supported by the cospectral measurements of Saddoughi and Veeravalli (1994) at higher Reynolds numbers. The square-root scaling suggests a mechanism which is more global than strict self-similarity based on local conditions, but the finite extent of the  $k^{-1}$  range suggest the opposite. More experimental results are needed in both cases.

The pay-off of this work should come in various ways. By far the most interesting would be the already discussed possibility of unifying the understanding of the large turbulent scales, which are at present considered non-universal and usually treated in separate ‘botanical’ ways. Some practical applications may also follow. Since these structures contain energy and Reynolds stresses, they are of practical importance, but their large size makes them expensive to compute. A quasi-linear model would open the way for their ‘super-grid’ modeling (S. Lele, personal communication). We have already mentioned that they probably control the low frequency noise from boundary layers.

This research has been supported in part by the Center for Turbulence Research and by AFOSR grant #F49620-97-1-0210. Partial support was also provided by the Spanish CICYT under contract PB95-0159, and by the European Commission program E980130118. I am indebted to P. Bradshaw, J. C. R. Hunt, A. E. Perry and V. Zakharov for illuminating discussions, and to J. Kim, R. D. Moser and S. Saddoughi for providing either unpublished or electronic versions of their data. A. A. Wray reviewed a early version of this manuscript and provided thoughtful comments.

## REFERENCES

- BETCHOV, R. & CRIMINALE, W. O. 1967 *Stability of parallel flows*, Academic Press.
- BULLOCK, K. J., COOPER, R. E. & ABERNATHY, F. H. 1978 Structural similarity in radial correlations and spectra of longitudinal velocity fluctuations in pipe flow. *J. Fluid Mech.* **88**, 585-608.

- CIMBALA, J. M. NAGIB, H. M. & ROSHKO, A. 1988 Large structure in the far wake of two-dimensional bluff bodies. *J. Fluid Mech.* **190**, 265-298.
- CLARK, J. A. & MARKLAND, E. 1971 Flow visualization in turbulent boundary layers. *Proc. Am. Soc. Civil Eng., J. Hydraulics Div.* **97**, 1635-1664.
- CHOI, H. & MOIN, P. 1990 On the space-time characteristics of wall-pressure fluctuations. *Phys. Fluids A*. **2**, 1450-1460.
- FARABEE, T. M. & CASARELLA, M. J. 1991 Spectral features of wall pressure fluctuations beneath turbulent boundary layers. *Phys. Fluids A*. **3**, 2410-2420.
- GASTER, M., KIT, E. & WYGNANSKI, I. 1985 Large-scale structures in a forced turbulent mixing layer. *J. Fluid Mech.* **150**, 23-39.
- HITES, M. H. 1997 Scaling of high-Reynolds number turbulent boundary layers in the National Diagnostic Facility. *Ph. D. Thesis*, Illinois Inst. of Technology.
- HUNT, J. C. R. 1984 Turbulence structure in thermal convection and shear-free boundary layers. *J. Fluid Mech.* **138**, 161-184.
- JEONG, J., HUSSAIN, F., SCHOPPA, W. & KIM, J. 1997 Coherent structures near the wall in a turbulent channel flow. *J. Fluid Mech.* **332**, 185-214.
- JIMÉNEZ, J. & MOIN, P. 1991 The minimal flow unit in near wall turbulence. *J. Fluid Mech.* **225**, 221-240.
- JIMÉNEZ, J. & PINELLI, A. 1998 The autonomous cycle of near-wall turbulence. Submitted, *J. Fluid Mech.*
- KIM, J., MOIN, P. & MOSER, R. D. 1987 Turbulence statistics in fully developed channel flow at low Reynolds number. *J. Fluid Mech.* **177**, 133-166.
- KOMMINAHO, J., LUNDBLADH, A. & JOHANSSON, A. V. 1996 Very large structures in plane turbulent Couette flow. *J. Fluid Mech.* **320**, 259-285.
- KROGSTAD, P-A., ANTONIA, R. A. & BROWNE, L. W. B. 1992 Comparison between rough- and smooth-wall turbulent boundary layers. *J. Fluid Mech.* **245**, 599-617.
- LAWN, C. J. 1971 The determination of the rate of dissipation in turbulent pipe flow. *J. Fluid Mech.* **48**, 477-505.
- LESSEN, M. 1978 On the power laws for turbulent jets, wakes and shearing layers and their relationship to the principle of marginal instability. *J. Fluid Mech.* **88**, 535-540.
- MANSOUR, N. N., MOSER, R. D. & KIM, J. 1996 Reynolds number effects in low Reynolds number turbulent channels, Case PCH10 in *AGARD AR-345*, 5-8
- NAGIB, H. & HITES, M. H. 1995 High Reynolds number boundary-layer measurements in the NDF. *AIAA Paper*. **95-0786**
- ORLANDI, P. & JIMÉNEZ, J. 1994 On the generation of turbulent wall friction. *Phys. Fluids A*. **6**, 634-641.
- PERRY, A. E. & ABELL, C. J. 1977 Asymptotic similarity of turbulence structures in smooth- and rough-walled pipes. *J. Fluid Mech.* **79**, 785-799.

- PERRY, A. E. & CHONG, M. S. 1982 On the mechanism of wall turbulence. *J. Fluid Mech.* **119**, 173-217.
- PERRY, A. E., HENBEST, S. & CHONG, M. S. 1986 A theoretical and experimental study of wall turbulence. *J. Fluid Mech.* **165**, 163-199.
- PERRY, A. E., LIM, K. L. & HENBEST, S. M. 1987 An experimental study of the turbulence structure in smooth- and rough-wall boundary layers. *J. Fluid Mech.* **177**, 437-466.
- PRIYMAK, V. G. & MIYAZAKI, T. 1994 Long-wave motions in turbulent shear flow. *Phys. Fluids.* **6**, 3454-3464.
- SANKARAN, R., SOKOLOV, M. & ANTONIA, R. A. 1988 Substructures in a turbulent spot. *J. Fluid Mech.* **197**, 389-414.
- SADDOUGHI, S. G. 1997 Local isotropy in complex turbulent boundary layers at high Reynolds number. *J. Fluid Mech.* **348**, 201-245.
- SADDOUGHI, S. G. & VEERAVALLI, S. V. 1994 Local isotropy in turbulent boundary layers at high Reynolds number. *J. Fluid Mech.* **268**, 333-372.
- TOWNSEND, A. A. 1976 *The structure of turbulent shear flows*, second ed., Cambridge U. Press.
- WALEFFE, F. 1997 On a self-sustaining process in shear flows. *Phys. Fluids.* **9**, 883-900.
- WUMAN, J. & WINSLOW, J. 1998 Intense sub-kilometer-scale boundary layer rolls observed in hurricane Fran. *Science.* **280**, 555-557.